Marine Pollution Bulletin 146 (2019) 631–638

Contents lists available at ScienceDirect

Marine Pollution Bulletin

journal homepage: www.elsevier.com/locate/marpolbul

On the use of random walk schemes in oil spill modelling

Tor Nordam[a,b,*], Raymond Nepstad[a], Emma Litzler[a], Johannes Röhrs[c]

[a] SINTEF Ocean, Trondheim, Norway
[b] Norwegian University of Science and Technology, Trondheim, Norway
[c] Norwegian Meteorological Institute, Oslo, Norway

ARTICLE INFO

Keywords:
Oil spill modelling
Random walk
Eddy diffusivity
Turbulent mixing
Vertical mixing

ABSTRACT

In oil spill models, vertical mixing due to turbulence is commonly modelled by random walk. If the eddy diffusivity varies with depth, failing to take the derivative of the diffusivity into account in the random walk scheme will lead to incorrect results. Depending on the diffusivity profile, the result may be either over- or underprediction of the amount of surfaced oil. The importance of using consistent random walk schemes has been known for decades in, *e.g.*, the plankton modelling community. However, it appears not to be common knowledge in the oil spill community, with inconsistent random walk schemes appearing even in recent publications. We demonstrate and quantify the error due to inconsistent random walk, using a simplified oil spill model, and two different diffusivity profiles. In the two cases considered, a commonly used inconsistent scheme predicts respectively 54% and 202% the amount of surface oil, compared to a consistent scheme.

1. Introduction

Oil spill modelling is commonly used during response operations and contingency planning. In both cases, the aim is to predict the destination of the oil, the amount at the surface, viable response options, etc. Modelling of the vertical distribution and surfacing of oil is a key aspect: Not only is the amount of oil at the surface in itself an important parameter that affects transport, stranding and response, but also the vertical distribution of submerged oil is important as this determines horizontal transport, due to current shear (Elliott, 1986).

Oil spill models commonly use a Lagrangian formulation, where the oil is represented by numerical particles (see, *e.g.*, Reed et al., 2000; French-McCay, 2004; Zelenke et al., 2012; De Dominicis et al., 2013; Röhrs et al., 2018). These particles are transported with wind, waves, and currents, and rise (or sink) due to buoyancy. Additionally, the particles are subject to a random walk process to model turbulent diffusion. The purpose of adding turbulent diffusion is to compensate for unresolved eddies in the current data; if included, these eddies would cause additional mixing. Horizontal and vertical diffusivity are commonly treated separately, due to the large difference in the scales involved. In this paper, we focus on the vertical direction, but the numerical scheme we discuss is equally applicable in the horizontal.

In the vertical direction, diffusivity can change by orders of magnitude across just a few meters. In wind-driven ocean surface boundary layers, vertical eddy diffusivity is largest in the interior of the mixing layer. Approaching the surface, the vertical turbulent diffusion is limited because the surface confines the size of turbulent eddies, and mixing efficiency is related to eddy size (Mellor and Yamada, 1982). This is commonly referred to as the law-of-the-wall, and for a flat interface the eddy diffusivity goes to zero at the surface. In the presence of surface waves, the law-of-the-wall does not apply exactly, however turbulent diffusion remains strongest at some depth away from the boundary (Craig and Banner, 1994).

Stable density gradients can also cause large changes in the eddy diffusivity. A strong pycnocline can act as a barrier, due to the energy required to lift the dense underlying water. Hence, the law-of-the-wall may hold approximately also at the base of the mixed layer, causing a large drop in eddy diffusivity over a distance of just a few meters or less (Gräwe et al., 2012).

An important principle in the modelling of diffusion is that a passive tracer which is initially well mixed should remain well mixed, regardless of the diffusivity profile (Lynch et al., 2014; Rodean, 1996; Thygesen and Ådlandsvik, 2007). This is known as the well-mixed condition (Thomson, 1987). The use of a consistent random walk scheme satisfying the well-mixed condition is essential. In the vertical direction, where persistent diffusivity gradients are present, an inconsistent random walk scheme can give large systematic errors. In the context of plankton modelling, Visser (1997) gives a particularly clear presentation of this issue. In the context of oil spill modelling, consistent random walk schemes have not received much attention in the

* Corresponding author.
E-mail address: tor.nordam@sintef.no (T. Nordam).

https://doi.org/10.1016/j.marpolbul.2019.07.002
Received 25 April 2019; Received in revised form 25 June 2019; Accepted 1 July 2019
Available online 23 July 2019
0025-326X/

literature. North et al. (2011) cite Visser (1997) for their vertical random walk scheme, but do not go into detail. Recent papers have pointed out the importance of using a consistent scheme, but do not quantify the error from using an inconsistent one (Boufadel et al., 2018; Röhrs et al., 2018).

In this paper, we demonstrate and quantify the errors that a commonly used inconsistent vertical random walk scheme can produce, compared to a consistent scheme. We describe the relevant theory of the random walk, and introduce a simple, one-dimensional oil spill model to investigate the effect of the random walk schemes. We simulate two example cases demonstrating that the choice of random walk scheme can have significant impact on the results.

2. Theory

As our starting point, we consider a one-dimensional system, where oil droplets submerged in the water column will rise due to buoyancy, and be randomly mixed due to eddy diffusivity. The oil droplets may reach the surface and form a slick, and surface oil may be re-submerged due to breaking waves. We assume that the concentration of oil droplets in the water column can be described by the advection-diffusion-reaction equation, with properly formulated boundary conditions and source terms.

In oil spill modelling, the standard approach is to model the advection-diffusion equation by a particle method, where numerical particles rise due to buoyancy, and diffusion is modelled as a random walk. This amounts to solving a stochastic differential equation (SDE), with a drift term representing buoyancy, and a noise term representing diffusion. Two different random walk schemes, corresponding to two different SDEs, are commonly seen in the literature. The first SDE is given by

$$\mathrm{d}z = w\,\mathrm{d}t + \sqrt{2K(z)}\,\mathrm{d}W(t). \tag{1}$$

Following Visser (1997), we refer to this as the naïve random walk. The second SDE, which we call the corrected random walk, is given by

$$\mathrm{d}z = (w + K'(z))\mathrm{d}t + \sqrt{2K(z)}\,\mathrm{d}W(t). \tag{2}$$

In both cases, $W(t)$ is a standard Wiener process (Kloeden and Platen, 1992, p. 40), $K(z)$ is the diffusivity as a function of depth, $K'(z)$ is its derivative with respect to z, and w is the rise speed due to buoyancy, which we here assume to be constant for a given particle.

As has been pointed out by numerous authors (see, *e.g.*, Hunter et al., 1993; Visser, 1997; Lynch et al., 2014; van Sebille et al., 2018), the naïve random walk is *not* equivalent to the advection-diffusion equation, except in the special case of constant diffusivity (*i.e.*, when $K'(z) = 0$ for all z). While this has been known in the plankton modelling community for two decades, it appears to be less well known in the oil spill modelling community. The mathematical and numerical details of random walk schemes have received limited attention in this field, and among those studies that do provide details, the naïve random walk scheme is still found in recent publications (see, *e.g.*, Wang et al., 2008; Lončar et al., 2012; Li et al., 2013; Liu and Sheng, 2014; Chen et al., 2015; De Dominicis et al., 2016; Yang et al., 2017).

2.1. Pseudovelocity

It can be shown (Hunter et al., 1993; Visser, 1997) that the naïve random walk described by Eq. (1) is equivalent to the Partial Differential Equation (PDE)

$$\frac{\partial C}{\partial t} = \frac{\partial^2}{\partial z^2}(K(z)C) - \frac{\partial}{\partial z}(wC). \tag{3a}$$

$$= \frac{\partial}{\partial z}\left(K(z)\frac{\partial C}{\partial z}\right) - \frac{\partial}{\partial z}(wC) + \frac{\partial}{\partial z}\left(\frac{\partial K}{\partial z}C\right). \tag{3b}$$

while the corrected random walk (Eq. (2)) is equivalent to the advection-diffusion equation in one dimension, which is:

$$\frac{\partial C}{\partial t} = \frac{\partial}{\partial z}\left(K(z)\frac{\partial C}{\partial z}\right) - \frac{\partial}{\partial z}(wC). \tag{4}$$

where $C(z,t)$ is the concentration. The link between Eqs. (1) and (3), and between Eqs. (2) and (4), is that C, when normalised, may be interpreted as the probability distribution for an ensemble of particles, whose trajectories are described by the SDE. Conversely, the concentration, C, may be found from the local density of particles (see, *e.g.*, Lynch et al., 2014, Chapter 8).

Comparing Eqs. (3b) and (4), we see that the additional last term in Eq. (3b) has the form of a drift term, $-\partial_z(vC)$, with $v = -K'(z)$, thus representing a transport away from regions of high diffusivity. Consequently, modelling a diffusion problem with the naïve random walk (Eq. (1)) does *not* solve the advection-diffusion equation, and will *not* obey the well-mixed condition (Hunter et al., 1993; Visser, 1997). The extra drift term $K'(z)\,\mathrm{d}t$ in Eq. (2) is called the pseudovelocity term (Lynch et al., 2014, p. 125), and compensates for the down-gradient diffusion bias which is present in Eq. (1). For details of how to arrive at Eq. (1) from Eq. (3), and at Eq. (2) from Eq. (4), see Appendix A.

2.2. Particle model

In order to investigate the effect of using the naïve random walk scheme in oil spill modelling, we formulate a simplified one-dimensional Lagrangian oil spill model. In this model, oil is represented by numerical particles, also called Lagrangian elements. Each particle represents a given mass of oil, and a single droplet size. Hence, a numerical particle with a small droplet size will represent a larger number of droplets (but the same mass) as a particle with a larger droplet size. In order to accurately represent a realistic droplet size distribution, a large number of particles is used.

The physics of the particle model is formulated as a series of steps. When repeatedly applied to a collection of particles, these steps describe the time evolution of the system under turbulent mixing, buoyant rise, surfacing and re-entrainment of oil droplets:

1 Randomly displace all submerged particles.
2 Any particles that were randomly displaced to a point above the surface (or below the sea bed) are reflected to an equal distance below the surface (or above the sea bed).
3 Move particles upwards due to buoyancy.
4 Any particles that were displaced to a point above the surface due to buoyancy are removed from the water column, and considered surfaced.
5 A surfaced particle may be resuspended into the water column with some probability, in which case it is placed at some random depth, and assigned a random droplet size.

As described in steps 1 and 3, we separate the random diffusion and the rise due to buoyancy into two different steps, with different handling of the boundary (steps 2 and 4). This is equivalent to solving the advection-diffusion equation with a reflecting boundary condition in diffusion, and an absorbing boundary condition in the buoyancy step (Nordam et al., 2019a).

The random displacement (step 1) is implemented by using the Euler-Maruyama scheme (Maruyama, 1955; Kloeden and Platen, 1992, page 305) to discretise the diffusion terms in Eqs. (1) and (2), yielding the following expression for the naïve scheme

$$z \to z + \sqrt{2K(z)}\,\Delta W. \tag{5}$$

and for the corrected scheme:

$$z \to z + K'(z)\Delta t + \sqrt{2K(z)}\,\Delta W. \tag{6}$$

In both cases, ΔW is a Gaussian random variable with expectation value $\langle \Delta W \rangle = 0$ and variance $\langle \Delta W^2 \rangle = \Delta t$. For an overview of other relevant SDE discretisation schemes in the context of marine particle transport, the interested reader is referred to Gräwe (2011).

For both schemes, the rise due to buoyancy (step 3) is given by

$$z \to z - w\Delta t. \tag{7}$$

where depth is positive downwards, and the rise speed, w, is found from Stokes' law at small Reynolds numbers, with a harmonic transition to a constant drag coefficient at higher Reynolds numbers (Johansen, 2000; Rye et al., 2008, p. 196):

$$w = \left(\frac{1}{w_1} + \frac{1}{w_2}\right)^{-1}. \tag{8a}$$

$$w_1 = \frac{d^2 g'}{18\nu_w}, \qquad w_2 = K_r\sqrt{d|g'|}\cdot\mathrm{sign}(g'). \tag{8b}$$

where d is the particle diameter, $g' = g(\rho_o - \rho_w)/\rho_w$ is the reduced gravity, $K_r = 1.054$ is an empirical constant, and the other variables are given in Table 1.

2.3. Entrainment

Oil droplets may be produced from a surface slick by breaking waves, and entrained into the water column (Delvigne and Sweeney, 1988; Johansen et al., 2015; Zeinstra-Helfrich et al., 2015). In step 5 of the model, we need to calculate the entrainment rate, the intrusion depth and the resulting droplet size distribution. These are all found from the sea state, and properties of the oil and seawater.

To predict the distribution of droplet sizes, we use the modified Weber number scaling developed by Johansen et al. (2015), which relates the ratio of characteristic droplet size to slick thickness, D/h, to the Reynolds and Weber numbers:

$$\frac{D}{h} = A\mathrm{We}^{-\alpha}\left[1 + B'\left(\frac{\mathrm{We}}{\mathrm{Re}}\right)^{\alpha}\right]. \tag{9}$$

where

$$\mathrm{We} = \frac{2gH_s\rho_o h}{\sigma_{ow}}, \qquad \mathrm{Re} = \frac{\sqrt{2gH_s}\rho_o h}{\mu_o}. \tag{10}$$

The constants A, B', and α in Eq. (9) are determined by fitting to experimental data; the values found by Johansen et al. (2015) are $A = 2.251$, $B' = 0.027$ and $\alpha = 0.6$. See Table 1 for definitions of the other parameters appearing here.

While the characteristic droplet size, D, can be predicted from Eq. (9), we additionally need to prescribe a droplet size distribution around this value. We differentiate between the *number* distribution, giving the number of droplets in a particular size interval, and the *volume* distribution, giving the volume of oil contained in a size interval.

Table 1
Parameters used in the simulations.

Acceleration of gravity	$g = 9.81\ \mathrm{m/s^2}$
Seawater density	$\rho_w = 1025\ \mathrm{kg/m^3}$
Seawater kinematic viscosity	$\nu_w = 1.36 \cdot 10^{-6}\ \mathrm{m^2/s}$
Oil density	$\rho_o = 992\ \mathrm{kg/m^3}$
Oil dynamic viscosity	$\mu_o = 1.51\ \mathrm{kg/m/s}$
Oil-water interfacial tension	$\sigma_{ow} = 13\ \mathrm{N/m}$
Initial oil film thickness	$h_0 = 3\ \mathrm{mm}$
Wind speed	$u = 12\ \mathrm{m/s}$
Wave height (from wind speed)	$H_s = 3.57\ \mathrm{m}$
Wave period (from wind speed)	$T_p = 9.95\ \mathrm{s}$
White-cap fraction (from wind speed)	$F_{bw} = 0.0225\ \mathrm{s^{-1}}$
Number of particles	$N_p = 1{,}000{,}000$
Timestep	$\Delta t = 0.1\ \mathrm{s}$
Simulation duration	$T_{max} = 6\ \mathrm{h}$

Following Johansen et al. (2015), we take the characteristic droplet size to signify the median droplet diameter of the number distribution, $D = d_{50}^n$, and use a log-normal distribution. As each numerical particle represents the same volume of oil, we need the *volume* droplet size distribution (for diameter d),

$$v(d) = \frac{1}{\sqrt{2\pi}\sigma}d^2\exp\left[-\frac{(\ln d - \mu)^2 - 9\sigma^4 - 6\mu\sigma^2}{2\sigma^2}\right]. \tag{11}$$

where we use a logarithmic standard deviation of $\sigma = 0.4$ (Johansen et al., 2015). The logarithmic mean μ is given by $d_{50}^v = \mathrm{e}^{\mu}$, and the relationship between the volume and number median diameters is (Johansen et al., 2015)

$$d_{50}^v = d_{50}^n + 3\sigma^2. \tag{12}$$

In step 5 in our model, the probability of a surface particle being entrained during an interval Δt is given by

$$p = 1 - \mathrm{e}^{-Q\Delta t}. \tag{13}$$

where Q is the entrainment rate. For calculation of entrainment rate, we use a model proposed by Li et al. (2017):

$$\frac{Q}{F_{bw}} = a\mathrm{We}^b\mathrm{Oh}^c. \tag{14}$$

Here, F_{bw} is the white-capping fraction per unit time, and

$$\mathrm{We} = \frac{gH_s\rho_w d_o}{\sigma_{ow}}, \qquad \mathrm{Oh} = \frac{\mu_o}{\sqrt{\rho_o\sigma_{ow}d_o}}. \tag{15}$$

Note that this definition of the Weber number is different from the one in Eq. (10). The length scale, d_o, is the Rayleigh-Taylor instability maximum droplet diameter, given by

$$d_o = 4\left(\frac{\sigma_{ow}}{(\rho_w - \rho_o)g}\right)^{1/2}. \tag{16}$$

The values of the empirical parameters appearing in Eq. (14) are $a = 4.604 \cdot 10^{-10}$, $b = 1.805$, and $c = -1.023$ (Li et al., 2017).

When submerged in step 5, a particle is assigned a droplet size drawn from the distribution described by Eq. (11), and new depth, drawn from a uniform distribution on the interval $H_s(1.5 \pm 0.35)$ (Delvigne and Sweeney, 1988).

A complete Python implementation of the simplified, one-dimensional oil spill model described above is available as open source[1] (Nordam et al., 2019b).

3. Example cases

To illustrate and quantify the importance of using a consistent random walk scheme in oil spill modelling, we consider a simplified, but realistic case. We have assumed a set of oil parameters corresponding to Troll crude, with an initial surface thickness of $h_0 = 3$ mm, and initially no submerged oil. We model the fraction of oil at the surface, as a function of time, and the concentration of submerged oil, as a function of depth and time. During the simulation, the remaining surface thickness, $h(t)$, is found by scaling h_0 with the fraction of oil at the surface. We assume a wind speed of 12 m/s, and from this we calculate the entrainment rate, intrusion depth, droplet size distribution and vertical diffusivity. A summary of the scenario parameters is given in Table 1.

3.1. Vertical diffusivity

We have used two different vertical eddy diffusivity profiles, which are shown in Fig. 1. Both diffusivity profiles describe conditions during

[1] github.com/nordam/Random-walk-in-oil-spill-modelling.

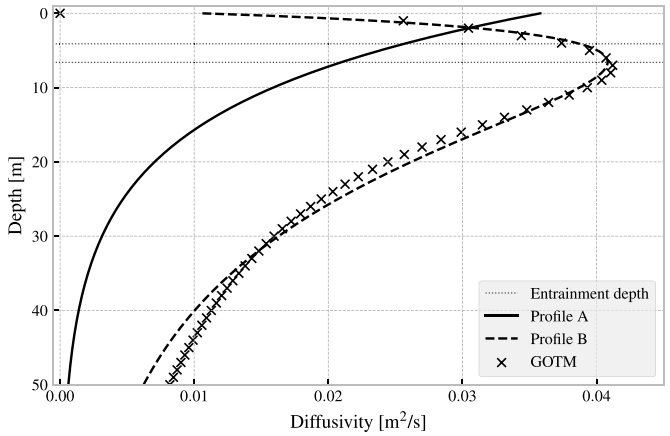

Fig. 1. The two diffusivity profiles used in the simulations. Profile A is found from Eq. (17), while profile B (Eq. (18)) is found by fitting an analytical expression to results from GOTM. The entrainment depth is indicated by the horizontal dotted lines.

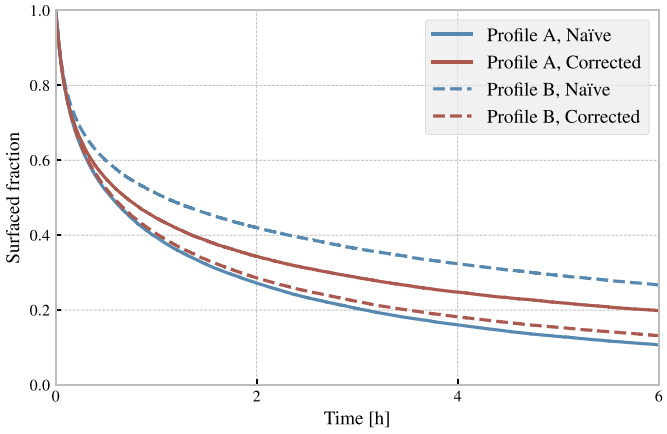

Fig. 2. Surfaced mass fraction of oil, as a function of time, for the two different random walk schemes. The results for Profile A are shown as continuous lines, and for Profile B as dashed lines.

forcing at a wind speed of 12 m/s, however they represent different degrees of approximation for the ocean surface layer dynamics.

Profile A assumes an exponentially decaying diffusivity, as applicable to the interior and lower base of the mixed layer. It has been used in oil spill and plankton modelling (see, *e.g.*, Skognes and Johansen, 2004; Tanaka and Franks, 2008; Li et al., 2013; Nordam et al., 2018), and is given by the empirical relationship (Ichiye, 1967):

$$K_A(z) = 0.028\frac{H_s^2}{T_p}\mathrm{e}^{-2kz}. \tag{17}$$

where z is depth (positive downwards), H_s and T_p are the significant wave height and the peak wave period, and k is the wave number. H_s and T_p can for example be derived from the wind speed using the JONSWAP spectrum and associated empirical relations (Carter, 1982), with the assumption of fully developed sea. Assuming deep water ($kL \gg 1$, where L is the water depth), the wave number can be found from the peak period by the dispersion relation $\omega^2 = gk$ (see, *e.g.*, Gill, 1982, p. 106). Note that the profile given by Eq. (17) does not reproduce the well-known behaviour of decreasing diffusivity towards the boundary at the surface. Still, the use of Eq. (17) may be a pragmatic choice in operational oil spill modelling, given that the input parameters can be derived from the wind speed.

Profile B is based on a prognostic model for turbulent kinetic energy (TKE) and a turbulent length scale, using the GOTM turbulence model (Umlauf et al., 2005), forced with a stress corresponding to wind speed of 12 m/s (Gill, 1982, p. 29). This profile is applicable in the near-surface, as well as the interior and base of the mixed layer. In this case, a k-ω turbulence closure with flux condition for TKE at the surface has been used, wherein the TKE flux at the surface accounts for wave breaking (Craig and Banner, 1994). This boundary condition is consistent with the idea that surface oil is entrained by breaking waves. The GOTM model setup and results are available online[2].

An analytical function has been fitted to the model results for easy vertical differentiation of the profile:

$$K_B(z) = \beta(z + z_0)\cdot\mathrm{e}^{-(\gamma\,(z+z_0))^\delta}. \tag{18}$$

where $\beta = 0.029$ m/s, $\gamma = 0.306$ 1/m, $\delta = 0.62$, $z_0 = 0.5$ m. Note that if a discrete diffusivity profile is to be used, it must be interpolated and differentiated in a consistent manner, to avoid numerical artifacts (see Appendix A and, *e.g.*, Ross and Sharples, 2004).

[2] github.com/nordam/Random-walk-in-oil-spill-modelling.

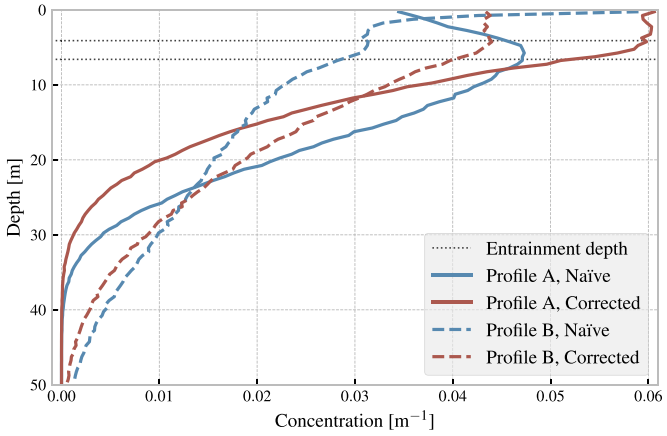

Fig. 3. Concentration of submerged oil after 6 hours, as a function of depth, for the two different random walk schemes. The results for Profile A are shown as continuous lines, and for Profile B as dashed lines. The entrainment depth is indicated by the horizontal dotted lines.

Table 2
Surfaced fraction, average depth, d_{50}^v, and d_{90}^v of the submerged oil, all after 6 hours.

	Surfaced	Depth	d_{50}^v	d_{90}^v
Profile A, naïve	0.107	11.5 m	355 μm	579 μm
Profile A, corrected	0.198	8.3 m	390 μm	679 μm
Profile B, naïve	0.267	15.3 m	434 μm	780 μm
Profile B, corrected	0.132	13.2 m	372 μm	627 μm

3.2. Results

In Fig. 2, we show the mass fraction of oil at the surface, as a function of time, for the naïve and the corrected random walk schemes, and for both diffusivity profiles (see Fig. 1). The results for Profile A are shown as continuous lines, and for Profile B as dashed lines. Fig. 3 shows the concentration of oil as a function of depth, after 6 hours, again for both schemes and both profiles. The concentration has been calculated by particle count in 100 bins, from 0 to 50 m depth. The surfaced fraction, along with the average depth, d_{50}^v, and d_{90}^v of the submerged oil (all after 6 hours), is given in Table 2.

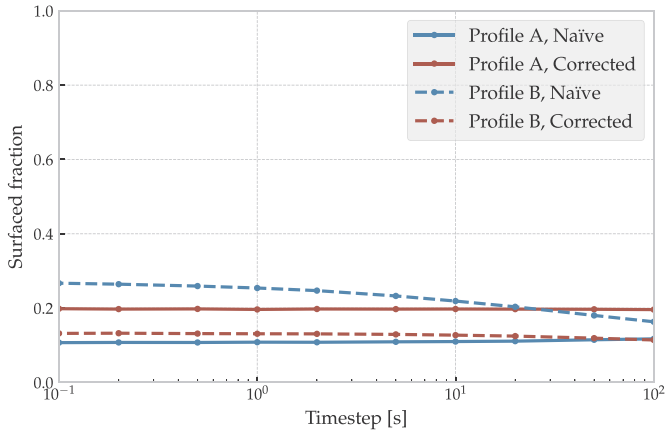

Fig. 4. Surfaced fraction after 6 hours, calculated for different timesteps.

4. Discussion

Correctly modelling turbulent mixing in the ocean is a highly non-trivial task. Describing mixing due to unresolved eddies as a diffusion process is in itself an approximation, and any chosen eddy diffusivity profile will be associated with considerable uncertainty. Nevertheless, if diffusion is to be modelled as a random walk with variable diffusivity, it should be done in a consistent manner to avoid systematic errors.

From the description of the pseudovelocity in Section 2.1, we conclude that the naïve random walk scheme can give incorrect results in oil spill modelling, as the spurious drift away from regions of high diffusivity interferes with the buoyant rise and surfacing of oil droplets. From the results presented above, we can quantify this effect by comparing the results of the naïve and corrected schemes.

For Profile A, the naïve scheme predicts about half as much oil at the surface after 6 hours as the corrected scheme, while for Profile B, the naïve scheme predicts about twice as much surfaced oil (see Fig. 2 and Table 2). The reason for these differences can be understood from the diffusivity profiles, shown in Fig. 1 together with the intrusion depth. In the interval where the entrained oil is distributed, the diffusivity given by Profile A decreases with depth, giving rise to a downwards drift in the naïve scheme, while Profile B is increasing with depth, giving an upwards drift.

Similar observations can be made from the concentration profiles shown in Fig. 3 and the depths given in Table 2. For Profile A, the naïve scheme predicts a larger amount of submerged oil, and the spurious downwards drift gives rise to larger predicted concentrations at greater depths, when compared to the corrected scheme. For Profile B, the results for the naïve scheme show less submerged oil in total, and the oil in the water column is pushed away from the region of high diffusivity, leading to larger concentrations both at the surface and at greater depth, compared to the corrected scheme. See also Appendix B for further discussion of the well-mixed condition.

We note also the difference in the d_{50}^{v} and d_{90}^{v} of the submerged droplets (Table 2). For Profile A, the distribution is shifted towards smaller droplets with the naïve scheme, as the spurious downwards drift is larger relative to the buoyancy for small droplets. For Profile B, the distribution is shifted towards larger droplets, as the smaller droplets are pushed towards the surface, reducing the amount of time they are kept in suspension by diffusion.

4.1. Choice of timestep

In order to verify that the results are independent of the timestep used, a convergence test was carried out. For both random walk schemes and both diffusivity profiles, the simulations were repeated with timesteps ranging from 100 s to 0.1 s. For each value of the timestep, we calculated the surfaced fraction after 6 hours. The results are shown in Fig. 4.

We first note that at a timestep of 0.1 s, the results all appear to have converged to stable values, and in particular the corrected scheme appears more or less converged at much longer timesteps. Visser (1997) proposed the following limit on the timestep:

$$\Delta t \ll \min \left| \frac{1}{K''(z)} \right|. \tag{19}$$

where the minimum is to be taken over the entire water column. If we calculate the limiting timestep from Eq. (19), we find 4219 s and 85.3 s for Profiles A and B respectively. It is generally agreed that the timestep should be kept at least an order of magnitude below this limit (Gräwe et al., 2012, Section 3.4), which seems to match our results for the corrected scheme. Note however that this did not have to be the case, due to an anomaly in the concentration field that may develop at the surface due to the reflecting boundary condition in diffusion (see, *e.g.*, Ross and Sharples, 2004; Nordam et al., 2019a). Furthermore, it is worth pointing out that the Visser timestep condition (Eq. (19)) can never be met if $K(z)$ is, *e.g.*, a step function, or otherwise has a discontinuous first derivative (see also Appendix A).

Finally, note that the results from the naïve scheme do *not* converge to those of the corrected scheme. This is as expected, and serves to demonstrate that the difference between the two schemes is not one of *accuracy*, but rather of *consistency*.

5. Conclusion

A recent paper by Boufadel et al. (2018) mentions that the use of a consistent random walk formulation may be important to correctly predict surfacing of small oil droplets. We have here quantified this effect, demonstrating that the naïve scheme can both over- and underpredict the amount of surfaced oil, depending on the vertical diffusivity profile. The reason is that the naïve scheme contains a drift away from regions of high diffusivity. Depending on the diffusivity profile, this spurious drift can be directed either upwards or downwards.

The error from using the naïve scheme is larger for small droplets, as their slow buoyant rise may be partially or completely dominated by the downgradient diffusion bias. Hence, the use of a consistent random walk scheme is even more important when dispersant application is considered. Using the naïve scheme, in particular in combination with an Ichiye-type diffusivity profile (see Eq. (17)), can lead to severe underprediction of the amount of re-surfacing in a surface dispersion operation.

Taking the derivative of the diffusivity profile into account is necessary to obey the well-mixed condition, and is a matter of using a random walk scheme which is consistent with the advection-diffusion equation. This is not related to the accuracy with which the “actual” diffusivity profile (or its derivative) is known. Once a diffusivity profile has been chosen for use in the model, its derivative has also been chosen, and failing to take it into account *will* lead to systematic errors.

Acknowledgments

The authors would like to gratefully acknowledge an anonymous reviewer of a previous paper, who politely objected to the notion of evaluating $K'(z)$ in an oil spill model. Without those comments, the current paper may not have been written.

Appendix A. Equivalence between SDE and PDE

Consider an Itô diffusion process described by the SDE

$$\mathrm{d}z = a(z,t)\,\mathrm{d}t + b(z,t)\,\mathrm{d}W. \tag{A1}$$

where $a(z,t)$ and $b(z,t)$ are "moderately smooth functions" (Kloeden and Platen, 1992, p. 37) (further conditions also apply, for details see, *e.g.*, Gihman and Skorohod (1972, pp. 96–102)). For this diffusion process, the Fokker-Planck equation for evolution of the transition probability density, $p(z_0,t_0,z,t)$, from an initial position z_0 at time t_0, to a position z at a later time t, is (Kloeden and Platen, 1992, p. 37):

$$\frac{\partial p}{\partial t} = \frac{1}{2}\frac{\partial^2}{\partial z^2}(b^2 p) - \frac{\partial}{\partial z}(ap). \tag{A2}$$

where we have dropped the arguments to a, b and p for brevity. Rewriting a bit, we get

$$\frac{\partial p}{\partial t} = \frac{1}{2}\frac{\partial}{\partial z}\left(b^2\frac{\partial p}{\partial z}\right) - \frac{\partial}{\partial z}\left[\left(a - \frac{1}{2}\frac{\partial b^2}{\partial z}\right)p\right]. \tag{A3}$$

We then compare Eq. (A3) to the advection-diffusion equation, with advection $w(z,t)$ and diffusion $K(z,t)$:

$$\frac{\partial C}{\partial t} = \frac{\partial}{\partial z}\left(K\frac{\partial C}{\partial z}\right) - \frac{\partial}{\partial z}(wC). \tag{A4}$$

By matching terms, and using that C is proportional to p, we find that $K = b^2/2 \Rightarrow b = \sqrt{2K}$, and $a = w + \partial_z K$. Hence, the SDE whose probability density is described by the advection-diffusion equation is the corrected random walk,

$$\mathrm{d}z = (w + K'(z))\,\mathrm{d}t + \sqrt{2K(z)}\,\mathrm{d}W. \tag{A5}$$

where $K'(z) = \partial_z K$. Note that since $a(z,t)$ and $b(z,t)$ in Eq. (A1) must be continuous, the equivalence with the advection-diffusion equation does not hold for, *e.g.*, step-function diffusivity, or piecewise linear diffusivity profiles with discontinuous first derivatives.

If instead we compare the Fokker-Planck equation (Eq. (A3)) to

$$\begin{aligned}\frac{\partial C}{\partial t} &= \frac{\partial^2}{\partial z^2}(KC) - \frac{\partial}{\partial z}(wC) \\ &= \frac{\partial}{\partial z}\left(K\frac{\partial C}{\partial z}\right) - \frac{\partial}{\partial z}\left[\left(w - \frac{\partial K}{\partial z}\right)C\right].\end{aligned} \tag{A6}$$

then by matching terms we find that $b = \sqrt{2K}$, and $a = w$. Hence, we see that the SDE whose probability density is described by Eq. (A6) is precisely the naïve random walk:

$$\mathrm{d}z = w\,\mathrm{d}t + \sqrt{2K(z)}\,\mathrm{d}W. \tag{A7}$$

As previously noted, Eq. (A6) is *not* identical to the advection-diffusion equation (Eq. (A4)), except in the special case of spatially constant diffusivity.

Appendix B. The well-mixed condition

The well-mixed condition (Thomson, 1987) states that an initially well mixed passive tracer undergoing diffusion (in a finite domain with no-flux boundary conditions), should remain well mixed, regardless of the diffusivity. That this must be so is immediately seen from the diffusion equation:

$$\frac{\partial C}{\partial t} = \frac{\partial}{\partial z}\left(K\frac{\partial C}{\partial z}\right). \tag{B1}$$

If $\partial_z C = 0$ everywhere (including at the boundaries), then we also have that $\partial_t C = 0$ everywhere, and no changes should occur.

To quantify the degree to which the naïve and corrected random walk schemes satisfy the well-mixed condition, we have simulated a passive tracer, initially evenly distributed on a domain from $z = 0$ m to $z = 50$ m. The simulations were carried out as described in Section 2.2, with zero rise velocity ($w = 0$), and the addition of a reflecting boundary at $z = 50$ m. We used both the previously presented diffusivity profiles (see Fig. 1), $N_p = 1{,}000{,}000$ particles, a timestep of $\Delta t = 0.1$ s, and the simulations were run for 48 hours.

We present two different metrics of the performance. First, in Fig. B.5, we present the concentration at the end of the simulation, as a function of depth, calculated by bin counts in 100 bins. Second, in Fig. B.6, we present the expectation value of the particle positions (*i.e.*, the first moment of the distribution, see, *e.g.*, Kloeden and Platen, 1992, p. 16). For a collection of uniformly distributed particles, on the interval from $z = 0$ m to $z = 50$ m, the expectation value of the particle positions is $\langle z\rangle = 25$ m. By the well-mixed condition, we know that this expectation value should remain unchanged. Hence, the error in the expectation value is a quantitative measure of the degree to which the well-mixed condition is satisfied. (Note, though, that a correct value of the first moment is a necessary, but not sufficient, condition for correct results. Only if all moments have the correct value is the modelled distribution equal to the true distribution.)

From the results in Fig. B.5, we observe that the naïve random walk gives a concentration profile with a minimum at the location of highest diffusivity, while the corrected random walk obeys the well-mixed condition (up to random fluctuations). From Fig. B.6, we similarly see that the corrected random walk gives $\langle z\rangle = 25$ m, as expected, while the naïve random walk causes the expectation value to change over time, as the distribution of particles is shifted downwards.

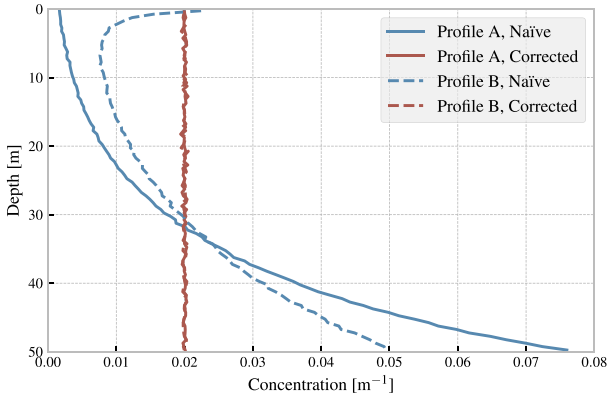

Fig. B.5. Concentration profiles for initially well-mixed passive tracer, after 48 hours. Concentrations are calculated from bin counts in 100 bins, with $N_p = 1{,}000{,}000$ particles, and a timestep of $\Delta t = 0.1$ s.

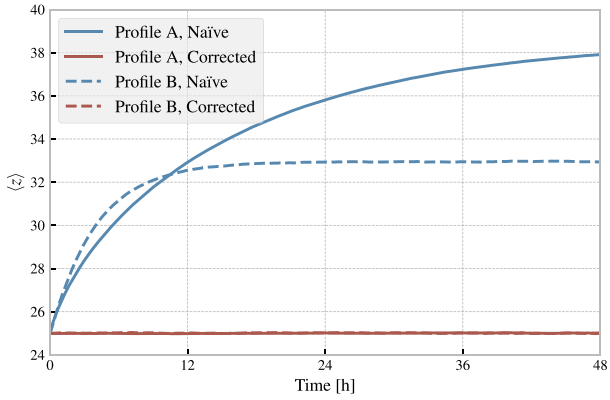

Fig. B.6. Expectation value of particle positions for initially well-mixed passive tracer, as a function of time, on the interval from $z = 0$ m to $z = 50$ m. The timestep was $\Delta t = 0.1$ s, and $N_p = 1{,}000{,}000$ particles were used.

References

Boufadel, M.C., Cui, F., Katz, J., Nedwed, T., Lee, K., 2018. On the transport and modeling of dispersed oil under ice. Mar. Pollut. Bull. 135, 569–580.

Carter, D., 1982. Prediction of wave height and period for a constant wind velocity using the JONSWAP results. Ocean Eng. 9, 17–33.

Chen, H., An, W., You, Y., Lei, F., Zhao, Y., Li, J., 2015. Numerical study of underwater fate of oil spilled from deepwater blowout. Ocean Eng. 110, 227–243.

Craig, P.D., Banner, M.L., 1994. Modeling wave-enhanced turbulence in the ocean surface layer. J. Phys. Oceanogr. 24 (12), 2546–2559.

De Dominicis, M., Bruciaferri, D., Gerin, R., Pinardi, N., Poulain, P., Garreau, P., Zodiatis, G., Perivoliotis, L., Fazioli, L., Sorgente, R., Manganiello, C., 2016. A multi-model assessment of the impact of currents, waves and wind in modelling surface drifters and oil spill. Deep-Sea Res. II Top. Stud. Oceanogr. 133, 21–38.

De Dominicis, M., Pinardi, N., Zodiatis, G., Lardner, R., 2013. MEDSLIK-II, a Lagrangian marine surface oil spill model for short-term forecasting — part 1: theory. Geosci. Model Dev. 6 (6), 1851–1869.

Delvigne, G., Sweeney, C., 1988. Natural dispersion of oil. Oil Chem. Pollut. 4 (4), 281–310.

Elliott, A.J., 1986. Shear diffusion and the spread of oil in the surface layers of the North Sea. Deutsche Hydrografische Zeitschrift 39 (3), 113–137.

French-McCay, D.P., 2004. Oil spill impact modelling. Environ. Toxicol. Chem. 23 (10), 2441–2456.

Gihman, I., Skorohod, A., 1972. Stochastic Differential Equations. Springer, Berlin Heidelberg New York.

Gill, A.E., 1982. Atmosphere-Ocean Dynamics. International Geophysics Series 30 Academic Press, New York.

Gräwe, U., 2011. Implementation of high-order particle-tracking schemes in a water column model. Ocean Model. 36 (1–2), 80–89.

Gräwe, U., Deleersnijder, E., Shah, S.H.A.M., Heemink, A.W., 2012. Why the Euler scheme in particle tracking is not enough: the shallow-sea pycnocline test case. Ocean Dyn. 62 (4), 501–514.

Hunter, J., Craig, P., Phillips, H., 1993. On the use of random walk models with spatially variable diffusivity. J. Comput. Phys. 106 (2), 366–376.

Ichiye, T., 1967. Upper ocean boundary-layer flow determined by dye diffusion. Phys. Fluids 10 (9), S270–S277.

Johansen, Ø., 2000. Deepblow-a Lagrangian plume model for deep water blowouts. Spill Sci. Technol. Bull. 6 (2), 103–111.

Johansen, Ø., Reed, M., Bodsberg, N.R., 2015. Natural dispersion revisited. Mar. Pollut. Bull. 93 (1), 20–26.

Kloeden, P.E., Platen, E., 1992. Numerical Solution of Stochastic Differential Equations. Springer-Verlag Berlin Heidelberg.

Li, Y., Zhu, J., Wang, H., 2013. The impact of different vertical diffusion schemes in a three-dimensional oil spill model in the Bohai Sea. Adv. Atmos. Sci. 30 (6), 1569–1586.

Li, Z., Spaulding, M.L., French-McCay, D., 2017. An algorithm for modeling entrainment and naturally and chemically dispersed oil droplet size distribution under surface breaking wave conditions. Mar. Pollut. Bull. 119 (1), 145–152.

Liu, T., Sheng, Y.P., 2014. Three dimensional simulation of transport and fate of oil spill under wave induced circulation. Mar. Pollut. Bull. 80 (1–2), 148–159.

Lončar, G., Leder, N., Paladin, M., 2012. Numerical modelling of an oil spill in the northern Adriatic. Oceanologia 54 (2), 143–173.

Lynch, D.R., Greenberg, D.A., Bilgili, A., McGillicuddy Jr, D.J., Manning, J.P., Aretxabaleta, A.L., 2014. Particles in the Coastal Ocean: Theory and Applications. Cambridge University Press.

Maruyama, G., 1955. Continuous Markov processes and stochastic equations. Rendiconti del Circolo Matematico di Palermo 4 (1), 48–90.

Mellor, G.L., Yamada, T., 1982. Development of a turbulence closure model for geophysical fluid problems. Rev. Geophys. 20 (4), 851–875.

Nordam, T., Kristiansen, R., Nepstad, R., Röhrs, J., 2019a. Numerical analysis of boundary conditions in a Lagrangian particle model for vertical mixing, transport and surfacing of buoyant particles in the water column. Ocean Model. 136, 107–119.

Nordam, T., Litzler, E., Rønningen, P., Aune, J., Hagelien, T.F., Loktu, A., Beegle-Krause, C.J., Brönner, U., 2018. Oil spill contingency and response modelling in ice-covered waters. In: Proceedings of the 41st AMOP Technical Seminar, Victoria, BC, Canada. Environment Canada, pp. 957–973.

Nordam, T., Nepstad, R., Litzler, E., Röhrs, J., 2019b. Nordam/random-walk-in-oil-spill-modelling (version v1.0). https://doi.org/10.5281/zenodo.2561055.

North, E.W., Adams, E.E., Schlag, Z., Sherwood, C.R., He, R., Hyun, K.H., Socolofsky, S.A., 2011. Simulating oil droplet dispersal from the deepwater horizon spill with a Lagrangian approach. In: Monitoring and Modeling the Deepwater Horizon Oil Spill: A Record Breaking Enterprise. Geophysical Monograph Series 195. American Geophysical Union, pp. 217–226.

Reed, M., Daling, P.S., Brakstad, O.G., Singsaas, I., Faksness, L.-G., Hetland, B., Ekrol, N.,

2000. OSCAR 2000: a multi-component 3-dimensional oil spill contingency and response model. In: Proceedings of the 23rd AMOP Technical Seminar, Vancouver, BC, Canada, pp. 663–680.
Rodean, H.C., 1996. Stochastic Lagrangian Models of Turbulent Diffusion. Meteorological Monographs 26 American Meteorological Society, Boston, MA.
Röhrs, J., Dagestad, K.-F., Asbjørnsen, H., Nordam, T., Skancke, J., Jones, C.E., Brekke, C., 2018. The effect of vertical mixing on the horizontal drift of oil spills. Ocean Sci. 14 (6), 1581–1601.
Ross, O.N., Sharples, J., 2004. Recipe for 1-D Lagrangian particle tracking models in space-varying diffusivity. Limnol. Oceanogr. Methods 2, 289–302.
Rye, H., Reed, M., Frost, T.K., Smit, M.G., Durgut, I., Johansen, Ø., Ditlevsen, M.K., 2008. Development of a numerical model for calculating exposure to toxic and nontoxic stressors in the water column and sediment from drilling discharges. Integr. Environ. Assess. Manag. 4 (2), 194–203.
Skognes, K., Johansen, Ø., 2004. Statmap–a 3-dimensional model for oil spill risk assessment. Environ. Model. Softw. 19 (7–8), 727–737.
Tanaka, Y., Franks, P.J., 2008. Vertical distributions of Japanese sardine (*Sardinops melanostictus*) eggs: comparison of observations and a wind-forced Lagrangian mixing model. Fish. Oceanogr. 17 (2), 89–100.
Thomson, D., 1987. Criteria for the selection of stochastic models of particle trajectories in turbulent flows. J. Fluid Mech. 180, 529–556.
Thygesen, U.H., Ådlandsvik, B., 2007. Simulating vertical turbulent dispersal with finite volumes and binned random walks. Mar. Ecol. Prog. Ser. 347, 145–153.
Umlauf, L., Burchard, H., Bolding, K., 2005. GOTM - Scientific Documentation: Version 3.2. Marine Science Reports Leibniz-Institute for Baltic Sea Research, Warnemuende, Germany.
van Sebille, E., Griffies, S.M., Abernathey, R., Adams, T.P., Berloff, P., Biastoch, A., Blanke, B., Chassignet, E.P., Cheng, Y., Cotter, C.J., Deleersnijder, E., Döös, K., Drake, H.F., Drijfhout, S., Gary, S.F., Heemink, A.W., Kjellsson, J., Koszalka, I.M., Lange, M., Lique, C., MacGilchrist, G.A., Marsh, R., Mayorga Adame, C.G., McAdam, R., Nencioli, F., Paris, C.B., Piggott, M.D., Polton, J.A., Rühs, S., Shah, S.H., 2018. Lagrangian ocean analysis: fundamentals and practices. Ocean Model. 121, 49–75.
Visser, A.W., 1997. Using random walk models to simulate the vertical distribution of particles in a turbulent water column. Mar. Ecol. Prog. Ser. 158, 275–281.
Wang, S.-D., Shen, Y.-M., Guo, Y.-K., Tang, J., 2008. Three-dimensional numerical simulation for transport of oil spills in seas. Ocean Eng. 35 (5), 503–510.
Yang, Y., Li, Y., Liu, G., Pan, Q., Wang, Z., 2017. A hindcast of the Bohai Bay oil spill during June to August 2011. Acta Oceanol. Sin. 36 (11), 21–26.
Zeinstra-Helfrich, M., Koops, W., Dijkstra, K., Murk, A.J., 2015. Quantification of the effect of oil layer thickness on entrainment of surface oil. Mar. Pollut. Bull. 96 (1–2), 401–409.
Zelenke, B., O'Connor, C., Barker, C., Beegle-Krause, C.J., Eclipse, L. E., 2012. General NOAA Operational Modeling Environment (GNOME), Technical Documentation, NOAA Technical Memorandum NOS OR&R 40.